

# Supporting Information for Publication

## STEM EDX Nitrogen Mapping of Nano-inclusions in Milky Diamonds from Juina, Brazil, Using a Windowless Silicon Drift Detector System

J. Rudloff-Grund<sup>\*</sup>, F.E. Brenker<sup>\*</sup>, K. Marquardt<sup>+</sup>, F.V. Kaminsky<sup>#</sup>, A. Schreiber<sup>§</sup>.

<sup>\*</sup> Geoscience Institute, Goethe University, Altenhoferallee 1, 60438 Frankfurt am Main, Germany

<sup>+</sup> Bayerisches Geoinstitut, University Bayreuth, Universitaetsstraße 30, 95447 Bayreuth, Germany

<sup>#</sup> KM Diamond Exploration Ltd., 2446 Shadbolt Lane, West Vancouver, British Columbia V7S 3J1, Canada

<sup>§</sup> Department 3.3 Chemistry and Physics of Earth Materials, GeoForschungsZentrum Potsdam, 14473 Potsdam, Germany

### Abstract

Supporting information includes more details on the ChemiSTEM™ Technology. Detailed information are given on the windowless design of silicon drift detectors (SDD), their placement within the transmission electron microscopy (TEM) column and differences between conventional Si(Li) detectors.

### Table of Content

<b>Chapter S-1 ChemiSTEM™ Technology</b>	<b>S-2</b>
<b>Chapter S-2 Comparison of the efficiency of a Super-X detector system with a conventional Si(Li) detector</b>	<b>S-3</b>
<i>S-2.1 Tilt response</i>	<i>S-3</i>
<i>S-2.2 The effect of beam current on the input count rate</i>	<i>S-4</i>
<i>S-2.3 Detection of light elements</i>	<i>S-4</i>
<i>S-2.4 Energy resolution</i>	<i>S-5</i>
<b>Chapter S-3 Results of Monte Carlo simulation of electron trajectory in solids (“CASINO”)</b>	<b>S-6</b>
<b>References</b>	<b>S-6</b>

## Chapter S-1 ChemiSTEM™ Technology

ChemiSTEM Technology consists of the FEI proprietary X-FEG high brightness Schottky field emission source and the FEI-designed Super-X™ system (Figure S-1). The compact design of the new developed SDDs allows integration up to four SDDs within the STEM column (Figure S-2). ChemiSTEM Technology includes fast mapping electronics capable of 100,000 spectra/second in EDX spectrum imaging. The integration of multiple SDDs results in a solid angle of 0.9 steradian (sr).

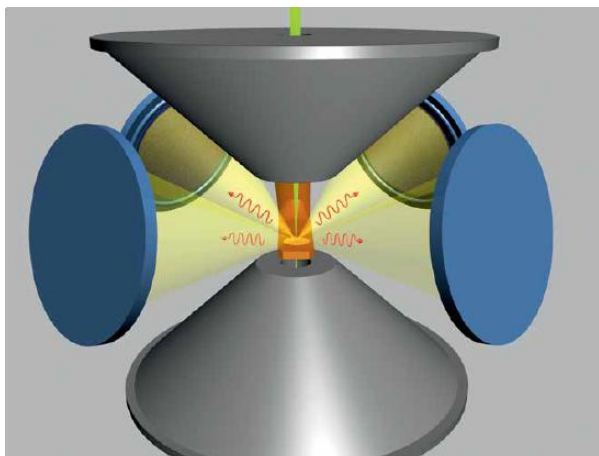


**Figure S-1.** Schematic illustration of ChemiSTEM™ design (Image courtesy of P. Schlossmacher, FEI Company). Four SDDs are symmetrically arranged around the optical TEM column.

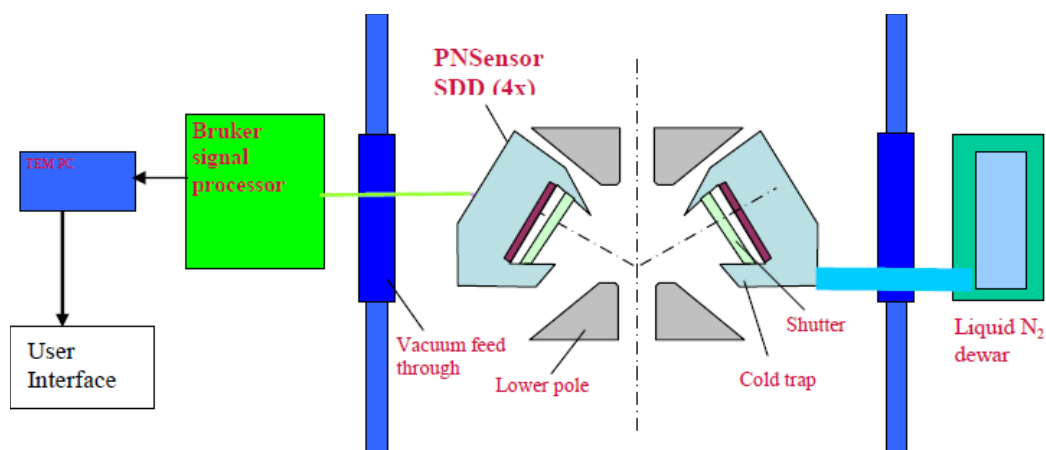


**Figure S-2.** Cross section through the TEM column near the objective lens<sup>2</sup> (Image courtesy of P. Schlossmacher, FEI Company). Two PNSensor designed SDDs are mounted around the specimen.

## Chapter S-2 Comparison of the efficiency of a Super-X detector system with a conventional Si(Li) detector

### S-2.1 Tilt response

Specimen tilting was a big disadvantage concerning single Si(Li) detector. Comparison of measured X-ray count rates with Super-X system (0.9 sr solid angle) over a tilt range from  $-25^\circ$  to  $+25^\circ$  and X-ray count rates detected by a conventional single Si(Li) detector (0.3 sr solid angle) clearly demonstrate the capabilities of the Super-X detector (Figure S-3). Super-X count rate always exceeds that of the single Si(Li) detector. Maximum count rate of the Super-X detector is achieved at zero degree tilt angle and never decreases more than 20 % over the entire tilt range. Maximum count rate of the Si(Li) detector can be observed at  $20^\circ$  tilt angle. Shadowing occurs at lower degrees and negatively affects the count rate. However, this is a general problem with single detectors, whether SDD or Si(Li) detector.

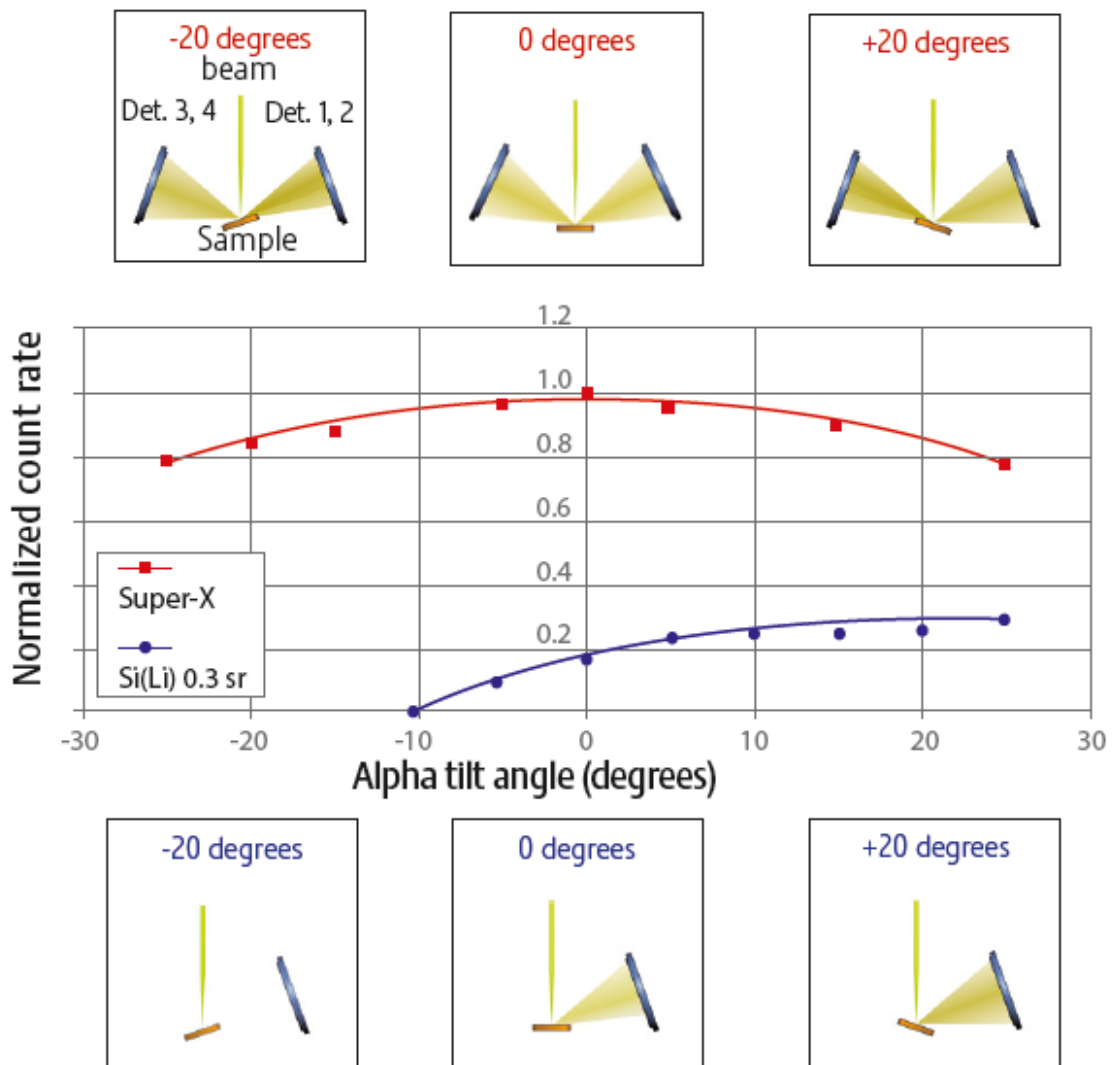


**Figure S-3.** Relative count rates of the Super-X system (red line) compared to that of a single Si(Li) detector (blue line) at different tilt angles<sup>1</sup> (Image courtesy of P. Schlossmacher<sup>1</sup>, FEI Company). Shadowing effects of the Super-X system and Si(Li) detector is presented above and below the count rate diagram respectively.

### S-2.2 The effect of beam current on the input count rate

Beam current positively correlates with the input count rate<sup>1</sup>. This effect is particularly important for the Super-X detector system (Figure S-4). The use of the Super-X system with a X-field emission gun (X-FEG) allows beam currents more than 10 nA resulting in a count rate of more than 400 000 counts per second without lowering the energy resolution<sup>1</sup>. This is in contrast to the capacity of a single Si(Li) detector in combination with a Schottky-FEG.

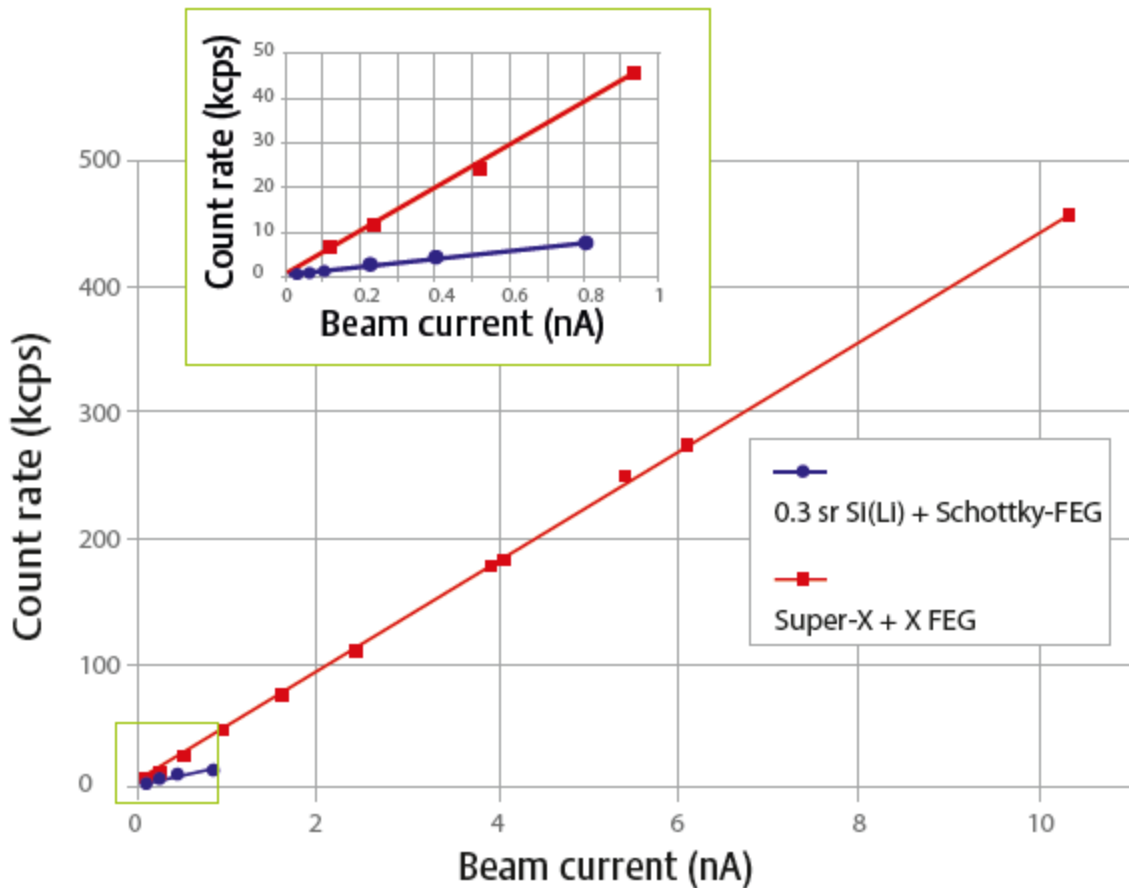


**Figure S-4.** Input count rate versus beam current for the Super-X detector system (red line) and a conventional Si(Li) detector (Image courtesy of P. Schlossmacher<sup>1</sup>, FEI Company).

### S-2.3 Detection of light elements

The windowless design of the Super-X detector system results in enhanced detection sensitivity for light elements such as nitrogen<sup>1</sup>. Figure S-5 demonstrate the advantage of the new system compared to a conventional single Si(Li) detector, especially in the low energy range (< 500 eV).

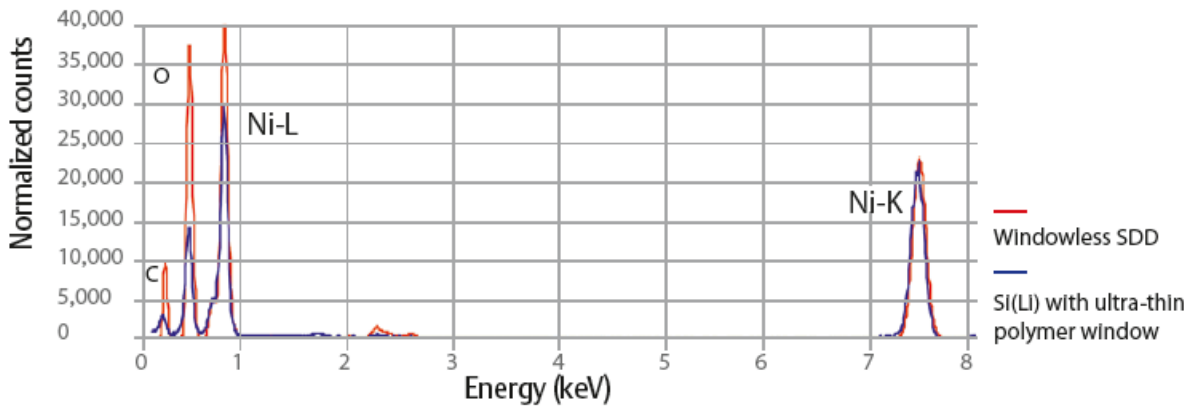


**Figure S-5.** Count rates detected by a windowless SDD compared to that of Si(Li) detector with ultra-thin polymer window (Image courtesy of P. Schlossmacher, FEI Company).

#### S-2.4 Energy resolution

Detector XFlash 5030 with an active area of 30 mm<sup>2</sup> achieves an energy resolution of  $\leq 127$  eV (Mn K $\alpha$ ) due to a special chip design with integrated charge amplifier. In contrast, energy resolution of a conventional Si(Li) detector decreases with increasing input count rate (Figure S-6).

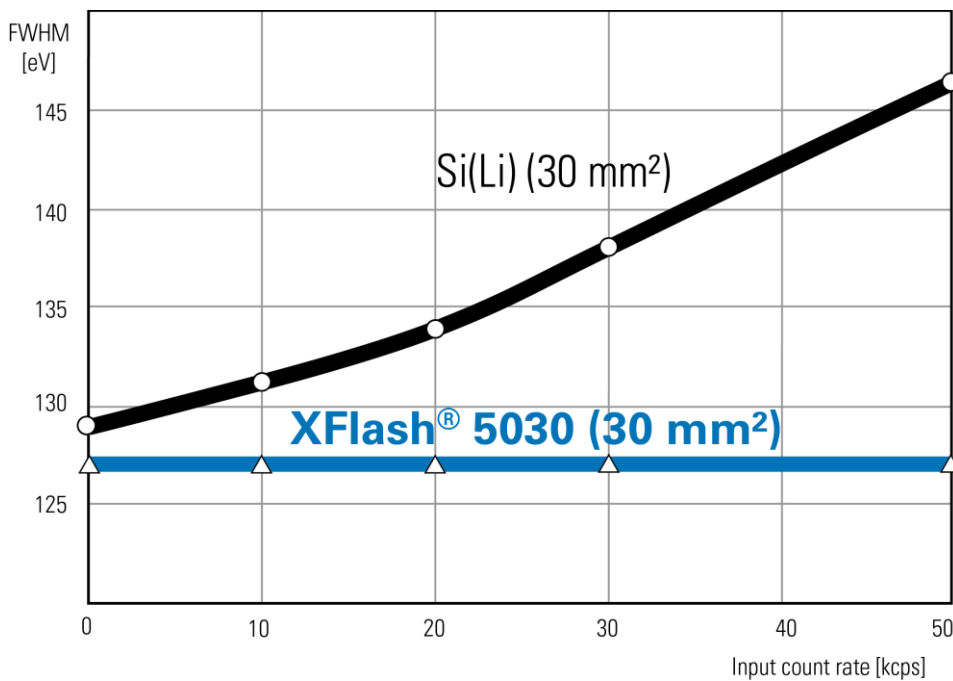


**Figure S-6.** Energy resolution at Mn K $\alpha$  versus input count rate of SDD XFlash 5030 (blue line) and Si(Li) (black line) (Image courtesy of Bruker).

### Chapter S-3 Results of Monte Carlo simulation of electron trajectory in solids (“CASINO”)

We simulated electron trajectories in a diamond using Version 2 of Monte Carlo simulation of electron trajectory in solids (“CASINO”) reprogrammed by Alexandre Réal Couture in 2000 under the supervision of Professor Dominique Drouin. The used spot size was 5 nm. The calculation was based on Rutherford formula. The result is shown in Figure S-7. The X-ray generation volume has a dimension of about 100 nm by 100 nm.

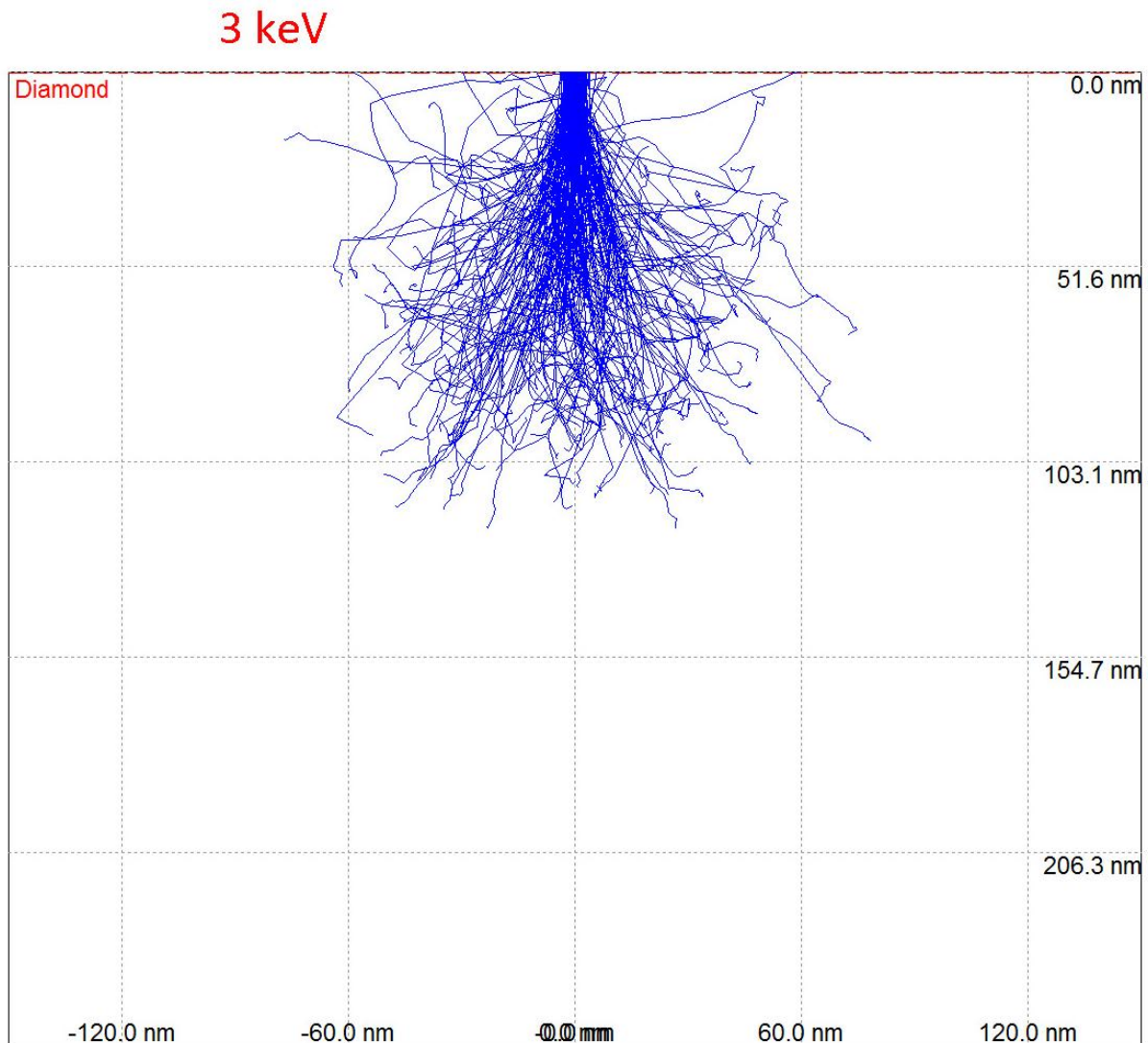


**Figure S-7.** Volume of generated X-rays calculated using Monte Carlo simulation for diamond at 3 keV.

#### References

- (1) Schlossmacher, P.; Klenov, D.O.; Freitag, B.; von Harrach, H.S. *Microscopy Today* **2010 a**, 18, 14–20.
- (2) Schlossmacher, P.; Klenov, D.O., Freitag, B.; von Harrach, S.; Steinbach, A. *Microscopy and Analysis* **2010 b**, 24, 5–8.